




Article

Compressive Strength of Conventional Glass Ionomer Cement Modified with TiO₂ Nano-Powder and Marine-Derived HAp Micro-Powder

Ana Ivanišević ¹, Valentina Brzović Rajić ^{1,*}, Ana Pilipović ², Matej Par ¹, Hrvoje Ivanković ³
and Anja Baraba ¹

¹ School of Dental Medicine, University of Zagreb, Gundulićeva 5, 10000 Zagreb, Croatia; aivanisevic@sfzg.hr (A.I.); mpar@sfzg.hr (M.P.); baraba@sfzg.hr (A.B.)

² Faculty of Mechanical Engineering and Naval Architecture, University of Zagreb, Lučićeva 5, 10000 Zagreb, Croatia; ana.pilipovic@fsb.hr

³ Faculty of Chemical Engineering and Technology, University of Zagreb, Marulićev trg 19, 10000 Zagreb, Croatia; hivan@fkit.hr

* Correspondence: vbrzovic.rajic@sfzg.hr; Tel.: +385-1-4802-126

Abstract: The aim of this research was to investigate the compressive strength (CS), breaking strength (BS), and compressive modulus (CM) of conventional glass ionomer cement (GIC) modified with TiO₂ nano particles, marine-derived hydroxyapatite (md-HAp) microparticles (<45 μm), and a combination of TiO₂ NP and md-HAp particles. The materials used in the study were conventional GIC Fuji IX GP Extra (GC Corporation, Tokyo, Japan), TiO₂ powder P25 (Degussa, Essen, Germany), and HAp synthesized from cuttlefish bone and ground in a mortar to obtain md-HAp powder. md-HAp was characterized using FTIR and SEM analysis. There were four groups of GIC samples: (i) Fuji IX control group, (ii) powder modified with 3 wt% TiO₂, (iii) powder modified with 3 wt% HAp, and (iv) powder modified with 1.5 wt% TiO₂ + 1.5 wt% HAp. Measurements were performed in a universal testing machine, and CS, BS, and CM were calculated. Statistical analysis was performed using ANOVA and Tukey's tests. CS, BS, and CM differed significantly between the Fuji IX control group and all experimental groups while differences between the experimental groups were not statistically significant. The addition of TiO₂ NP, md-HAp micro-sized particles, and a combination of TiO₂ and md-HAp reduced the CS, BS, and CM of conventional GICs when mixed at the powder/liquid (p/l) ratio recommended by the manufacturer.



Citation: Ivanišević, A.; Rajić, V.B.; Pilipović, A.; Par, M.; Ivanković, H.; Baraba, A. Compressive Strength of Conventional Glass Ionomer Cement Modified with TiO₂ Nano-Powder and Marine-Derived HAp Micro-Powder. *Materials* **2021**, *14*, 4964. <https://doi.org/10.3390/ma14174964>

Academic Editor: Ștefan Țălu

Received: 28 July 2021

Accepted: 28 August 2021

Published: 31 August 2021

Publisher's Note: MDPI stays neutral with regard to jurisdictional claims in published maps and institutional affiliations.



Copyright: © 2021 by the authors. Licensee MDPI, Basel, Switzerland. This article is an open access article distributed under the terms and conditions of the Creative Commons Attribution (CC BY) license (<https://creativecommons.org/licenses/by/4.0/>).

Keywords: glass ionomer cement; compressive strength; titanium dioxide; hydroxyapatite

1. Introduction

Glass ionomer cements (GICs) were invented by Wilson and Kent more than 50 years ago and introduced into dentistry as translucent cements [1]. GICs are two-component materials containing a fluoro-aluminosilicate powder and an aqueous solution of organic polyalkenoic acids, predominantly polyacrylic acid. After mixing the two components, GICs are set by the neutralization reaction between the polyalkenoic acids and metal oxides from fluoro-aluminosilicate glass particles to form insoluble polysalts and water [2]. The cross-linking of the polyacrylate chains with metal ions (calcium and aluminum) forms a matrix in which glass particles are enclosed [2]. The cross-linking ensures the strength, stiffness, and insolubility of the cements, and is influenced by the characteristics of the GIC material's components (polyacid and powder composition), powder-to-liquid ratio, and the environmental conditions in which the setting occurs [3,4]. The favorable properties of GIC materials are their ability to chemically bind to enamel and dentin, anticariogenic activity through the release of fluoride ions, and biocompatibility. These properties have made them widely accepted for use in clinical dentistry as luting materials, cavity liners, and restorative materials [2,3]. Besides in dentistry, GICs have been found useful even in

neuro-otological surgeries and reconstruction surgeries of the maxillofacial region due to their biocompatibility and adhesion to bone structure [5–7].

Despite these favorable characteristics, GICs do have certain disadvantages, including inferior physical properties—relatively low compressive strength, brittleness, and poor wear characteristics [8]. To improve their inferior physical properties, GICs have undergone various modifications, including increased powder/liquid (p/l) ratio, different particle sizes, and modification with resin [9,10]. Moreover, several materials have been proposed as GIC additives to enhance physical properties, including titanium dioxide (TiO₂), hydroxyapatite (HAp), and others [11–13]. HAp is a major calcified component of bone and hard dental tissues. When added to the GIC powder, HAp was reported to interact with carboxylate groups of polyacids, thus improving cross-linking and hardness of the cement [14,15]. Marine-derived HAp was shown to be biocompatible, readily available, and low cost [16]. Furthermore, titanium dioxide (TiO₂) is a chemically stable, biocompatible inorganic additive exhibiting antibacterial properties. TiO₂ nano particles (NP) were shown to have antibacterial effects and to potentially reinforce GICs [11,17]. The microhardness, flexural and compressive strength, and antibacterial activity of TiO₂ NP-modified GICs were found to be improved without interfering with adhesion to mineralized dental tissues and with fluoride release. The improvement was more pronounced at 3% (*w/w*) than at 5% and 7% (*w/w*) [11]. Although there are some concerns about the potentially cytotoxic effects of TiO₂ NP, its toxicity is generally considered to be low [18,19]. The combination of HAp and TiO₂ has been used for coating titanium implants with improved osteogenic activity around the implants [20]. According to the available literature, there have been no studies dealing with the mechanical properties of GICs after simultaneous addition of HAp and TiO₂ NP.

Based on previous reports, we expected that supplementing TiO₂ NPs and HAp micro-sized particles into GIC would enhance the mechanical properties. The objective of this research was to investigate the compressive strength (CS), breaking strength (BS), and compressive modulus (CM) of conventional GIC (Fuji IX) modified with 3% (*w/w*) TiO₂ NP, 3% (*w/w*) md-HAp, and combined 1.5% (*w/w*) TiO₂ + 1.5% (*w/w*) md-HAp.

2. Materials and Methods

A commercially available conventional GIC was used in this study: Fuji IX GP Extra (GC Corporation, Tokyo, Japan). Commercial TiO₂ powder P25 was also used (Degussa, Essen, Germany). The specifications of the TiO₂ were: mineral composition 85% rutile and 15% anatase, purity 99.9%, average size of primary particles 20 nm, molar mass 79.87 g/mol, density 4.26 g/cm³. Hydroxyapatite powder was synthesized from cuttlefish bone [21], ground in a mortar and sifted through a 45 µm sieve, resulting in the HAp powder with particles <45 µm (Figure 1).

2.1. Characterization of md-HAp Using Fourier Transform Infrared (FTIR) Spectroscopy

Fourier-transform infrared (FTIR) spectroscopy was performed on the marine-derived HAp powder and an analytical grade HAp powder (Merck, Darmstadt, Germany). The diamond attenuated total reflectance (ATR) accessory of Nicolet iS50 FTIR spectrometer (Thermo Fisher Scientific, Waltham, MA, USA) was covered with 0.05 g of the powder, which was gently distributed and pressed on the diamond ATR crystal using a modified accessory press. FTIR spectra were collected in absorbance mode using a mercury-homogenous cadmium-telluride detector (spectral range: 3500–400 cm⁻¹, resolution: 4 cm⁻¹, number of scans per spectrum: 20). The assignments of FTIR spectral bands were performed according to Figueiredo et al. [22].

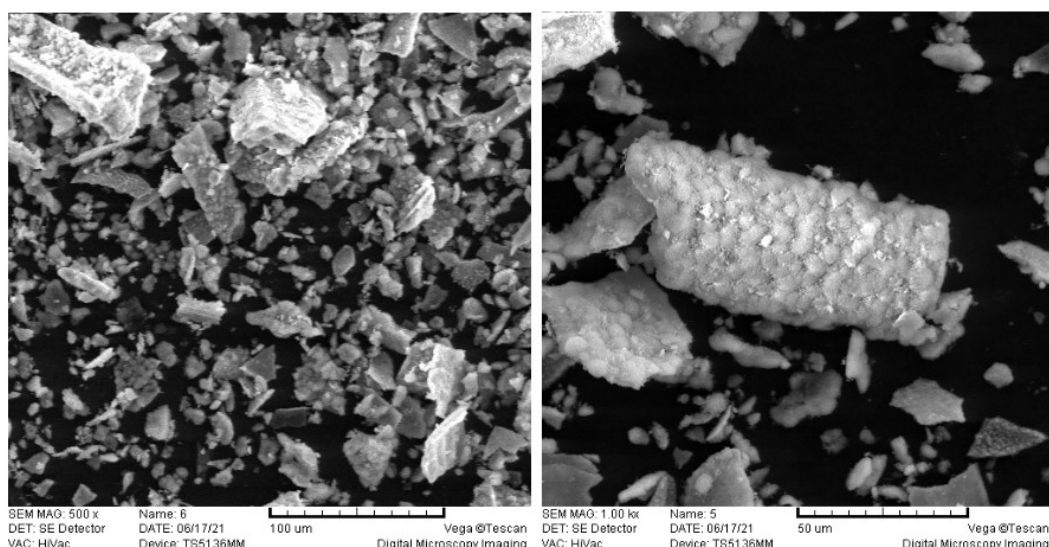


Figure 1. SEM images of md-HAp powder at magnifications of 500× and 1000×. md-HAp was ground in a mortar and sifted through a 45 µm sieve resulting in the powder composed of angular particles <45 µm.

2.2. Preparation of Samples and Determining Mechanical Properties

The fluoro-aluminosilicate glass powder of commercial GIC, HAp powder, and TiO₂ powder were manually mixed with a mortar and pestle for 10 min to obtain as homogenous a distribution as possible of HAp and/or TiO₂ in the Fuji IX fluoro-aluminosilicate glass powder. The prepared powders were then mixed with the liquid component by plastic spatula, according to the manufacturer's instructions, at a recommended powder/liquid ratio of 3:6. Four groups were prepared—a control group without any particles added and three experimental groups in which the powder was modified with 3 wt% TiO₂, 3 wt% HAp, and 1.5 wt% TiO₂ + 1.5 wt% HAp.

For CS, BS, and CM testing, cylinder-shaped samples were made for each group ($N = 4$). After mixing, the material was instilled into silicone moulds (4 mm diameter × 8 mm height) using a syringe (Centrix, Shelton, CT, USA). Polyester strips were placed on both sides of the mould, and the material was gently compressed. The samples were left for 1 h to harden. The samples were then removed from the silicone mould and kept in deionized water for a week. After complete setting, the samples were polished in steel moulds on a grinder-polisher (Buehler, IL, USA) using 500-grit carbide paper under continuous water rinsing. Final dimensions of the samples for compressive strength testing were 4 mm diameter and 6 mm height.

The measurements were performed according to ISO specification 7489:1986 [23] at a speed of 0.75 mm/min, room temperature of 22 °C, and relative humidity of 45% (Figure 2). The CS of each specimen, expressed in N/mm², was calculated using the equation:

$$CS = \frac{4 \cdot F}{\pi \cdot d^2} \quad (1)$$

where F (N) is the max. force and d (mm) is the diameter of the specimen.

Compression breaking strength was calculated by the same equation; only the value of the force at the moment of breaking of the test specimen was used in the calculation.

Compression modulus E_c is calculated according to the equation:

$$E_c = \frac{\sigma}{\varepsilon} = \frac{\sigma_2 - \sigma_1}{\varepsilon_2 - \varepsilon_1} \quad (2)$$

where E_c (N/mm²) is compression modulus, σ (N/mm²) is stress, and ε (%) is strain.

In this testing, stress values were taken from $\sigma_2 = 40$ N/mm² and $\sigma_1 = 20$ N/mm², and for these values, their deformations were read.

The data were statistically analysed using descriptive analysis, a one-way ANOVA, and a post-hoc Tukey's test at a level of significance $p = 0.05$. Normality of distribution was tested using the Shapiro-Wilk test. Levene's test was used for equality of variances testing, and in the case of non-homogeneous variances, the Welch's variant of ANOVA test was used.

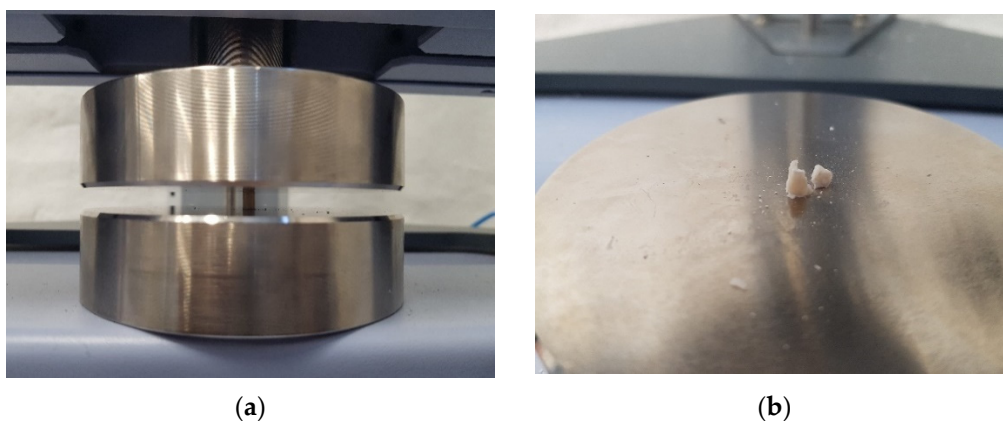


Figure 2. The testing procedure (a) and the specimen after testing (b).

3. Results

3.1. FTIR Analysis of md-HAp

Spectra of md-HAp powder and pure hydroxyapatite were recorded and compared. The bands at 560, 600, and 1012 cm^{-1} correspond to the vibrations of the PO_4 group and are characteristic of hydroxyapatite. Additionally, the bands at 1450 and 1410 cm^{-1} in md-HAp correspond to the organic part (CH_2) and the carbonate group (Figure 3). FTIR spectra thus showed that the md-HAp powder consisted of carbonated hydroxyapatite with some organic (protein) content [22].

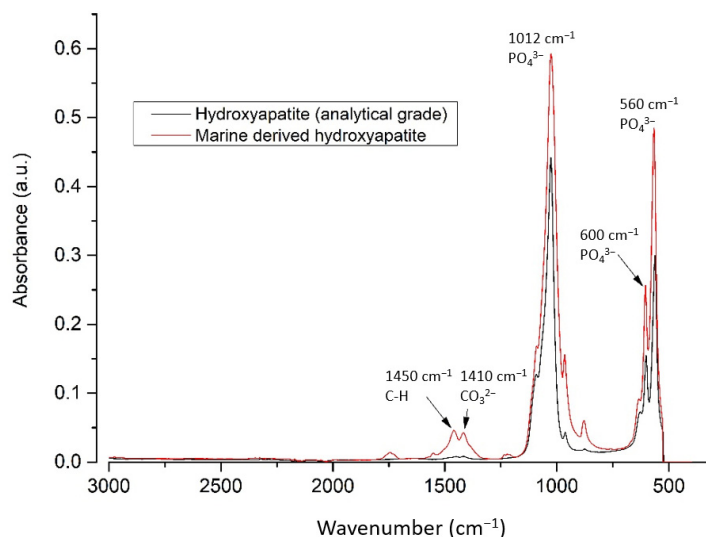


Figure 3. Spectra of analytical grade HAp and md-HAp showed a high degree of concordance.

3.2. Mechanical Properties of the GIC Samples

The dimensions of the samples (4 mm \times 6 mm) between the four experimental groups did not significantly differ (ANOVA, $p > 0.05$ for diameter and height).

The compression stress-strain diagram for the four groups of samples is shown in Figure 4. The diagram shows mean curves (mean values are shown in Table 1) per batch. The force and displacement were recorded every 0.1 s until the test specimen broke. After that, the strength and strain values were calculated from these data according to

Equations (1) and (2), and the mean values were calculated. At smaller load, the stress-strain curve is flatter and has higher displacement (initial loading) until the surface of the sample gets aligned to the surface of the testing machine's jaw.

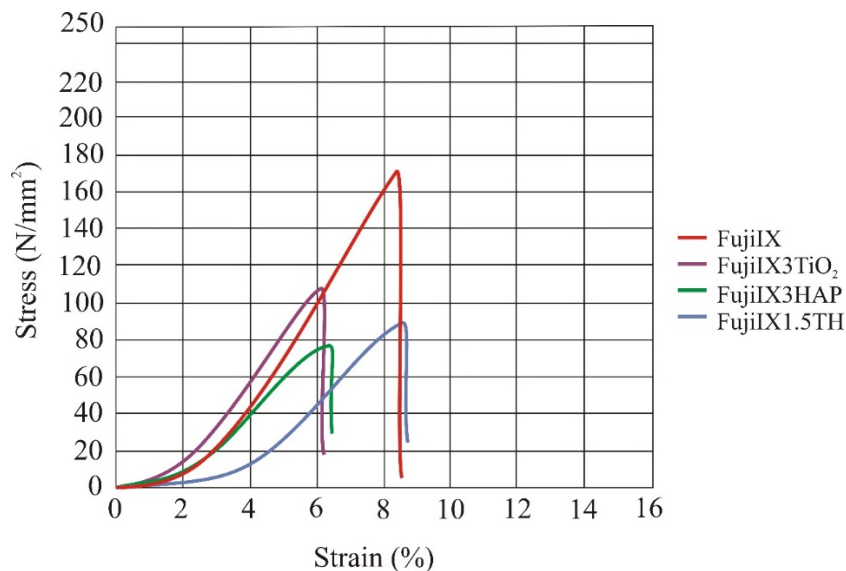


Figure 4. Compression stress–strain diagram. The mean values for the four groups of materials ($N = 6$) are shown in the diagram. The control group in which Fuji IX was not modified exhibited the highest compressive stress and compressive strength. Legend: FujiIX is a control group, FujiIX3TiO₂ is material with 3% of TiO₂, FujiIX3HAP is material with 3% HAP and FujiIX1.5TH material with 1.5% of TiO₂ and 1.5% of HAP.

Table 1. Mean values and standard deviations (sd.) of compressive strength, breaking strength, deformation at break, and compressive modulus for the four Fuji IX groups.

Mechanical Property	0% TiO ₂ 0% HAP		3% TiO ₂		3% HAP		1.5% TiO ₂ 1.5% HAP		ANOVA
	Mean	sd.	Mean	sd.	Mean	sd.	Mean	sd.	<i>p</i>
Compressive strength (N/mm ²)	172.71	(17.15)	109.23	(14.72)	78.52	(15.49)	91.01	(10.85)	<0.0001 ^a
Breaking strength (N/mm ²)	170.25	(18.45)	108.26	(14.57)	75.70	(16.02)	86.59	(12.76)	<0.0001 ^a
Deformation at break (%)	8.50	(1.49)	6.17	(0.61)	6.41	(0.51)	8.64	(1.95)	0.03
Compressive modulus (N/mm ²)	2955.91	(98.30)	2343.39	(195.60)	1747.29	(268.45)	1886.06	(267.68)	<0.0001 ^a

^a Difference between control group and experimental groups with modified powder was statistically significant.

The results for compressive strength, breaking strength, and compressive modulus for the Fuji IX control and the three experimental groups are given in Table 1.

Statistical analysis showed that the differences between the four groups were statistically significant for all mechanical properties measured (ANOVA test). Individual comparisons between the groups using Tukey's test showed that the compressive strength, breaking strength, and compressive modulus differed significantly between Fuji IX control group and all experimental groups (modified with 3 wt% HAP, 3 wt% TiO₂, and 1.5 wt% HAP + 1.5 wt% TiO₂), while the differences between the experimental groups were not statistically significant. The mean values of deformation at break differed between the groups ($p = 0.03$),

4. Discussion

The results of the present study revealed that the modification of a conventional GIC powder with nano particles of TiO₂ and micro particles of md-HAP (<45 μm) did

not improve compressive strength, compressive modulus, and breaking strength. On the contrary, the tested mechanical properties deteriorated, and in some cases, significantly. The hypotheses assumed enhanced compressive strength, compressive modulus, deformation break, and breaking strength among the modified materials, and were thus rejected.

Compressive and flexural tests are used to simulate the stress applied to materials used in clinical dentistry. Most mastication forces are compressive in nature, and compressive tests reveal the critical value at which the material breaks/fails during mastication. The minimum value necessary to resist the masticatory forces in the posterior teeth would be 125 MPa, while it would be 100 MPa for primary dentition [24,25]. This implies that the samples from the experimental groups with modified FAS powders do not have sufficient compressive strength to resist forces in the posterior region.

The addition of 3% (*w/w*) TiO₂ significantly reduced the compressive strength of Fuji IX as well as the breaking strength and compressive modulus. This result is not in accordance with the results of previous studies [11,18]. The reason for this was perhaps because the p/l ratio was unchanged in the experimental powder modified with nanoparticles of TiO₂. In a previous study, the original p/l ratio was reduced when the original FAS powder was replaced with nano FAS powder because of the low bulk density of the nano-sized powder [26]. Although in our study the original GIC powder was modified with only 3 wt% TiO₂ NP, the reduction of mechanical properties could be explained by the overall lower bulk density of the modified powder. Moreover, since p/l ratio was shown to influence mechanical properties [3], the intention was to have the p/l ratio the same in all groups so that the influence of the powders' composition on mechanical properties would be the sole variable. TiO₂ NP between the larger FAS glass particles can also interact with polyacrylic acid [27], but it might be that the carboxylic groups were insufficient to react with the high surface to volume ratio TiO₂ particles, so the interfacial bonding was weaker between the particles and the cement matrix. The unfavourable results after mixing TiO₂ NP might be different if nanotubes were used, similar to the study by Cibim et al. [28].

Modification with 3% (*w/w*) md-HAp powder also reduced mechanical properties. CS was even lower than with modification with 3% (*w/w*) TiO₂ NP. It was previously suggested that the HAp particles dispersed in FAS react with polyalkenoic acid similarly to HAp from dentin and enamel: the ionic attraction between carboxyl groups from GIC and the calcium ions in the HAp of enamel and dentine results in the displacement of calcium and phosphate ions from the HAp and the formation of an ion-exchange layer of calcium and aluminium phosphates and polyacrylates at the interface [2,29–31]. These additional matrix layers should improve mechanical properties. Since this was not the case in the present study, apparently these additional intermediate strengthening ionic attractions did not occur. Perhaps the HAp micro-sized particles were too big (<45 µm). Indeed, larger particles have a relatively smaller specific surface area, and there are fewer metal ions from the modified powder leaching into the ion exchange layer to form bonds. Furthermore, the wide distribution of particle sizes in GIC powder ensures a high packing density, and for optimal strength, the particles should be neither too fine nor too large [32,33]. The original Fuji IX powder contains angular particles whose size ranges from 0.3 to 200 µm, 36.91% are <5.0 µm and 51.72% are of sizes from 5.0 to 50 µm [26,33]. The addition of HAp particles <45 µm changed the ratio between the larger and fine particles, lowering packing density and negatively affecting mechanical properties. Furthermore, besides the size and distribution of the particles, the p/l ratio influences the strength. Experimental cements modified with HAp micro-sized particles had high bulk density and were oversaturated at 3:6 p/l ratio, compromising ionic interaction between HAp and carboxylic groups and cross-linking. In short, fewer ions and bonds and a higher number of unreacted particles could explain the lower strength of the experimental cements in the present study.

Moreover, the tested mechanical properties might have been reduced due to the protein content in md-HAp and carbonated HAp. This might imply that the synthetic HAp of high purity should be preferred as an additive to FAS powder, rather than the HAp

derived from fish waste, although HAp and collagen derived from fish waste have shown promising results in bone tissue engineering [16].

Since GICs are also used in reconstruction surgeries, along with improved mechanical properties, the addition of components favouring osteointegration would be desirable. TiO₂ and HAp coatings improved osteointegration of titanium implants [20]. However, the present study suggests that the combination of 1.5% (*w/w*) TiO₂ NP and 1.5% (*w/w*) HAp did not improve compressive strength, breaking, and compressive modulus when added to Fuji IX powder, most likely due to the same reason pointed out earlier—that the p/l ratio of 3:6 was not optimal for the cement with the powder modified with the combination of the two particles.

Manual spatulation of the modified powders was harder than in the case of control samples. The recommended p/l ratio was harder to achieve, especially in the case of modification with TiO₂ NP, due to the lower bulk density of the powder. It was harder to manipulate with the mixed cement, leading to more air inclusions, which also reduced mechanical properties. Hand mixing could be taken as a limitation of the present study. However, compressive strength values of control samples are in the range of the reported values for Fuji IX [34], so we cannot attribute the lower results in the experimental groups solely to the imperfection of manual mixing since all the samples were mixed in the same manner.

5. Conclusions

Combined and individual incorporation of TiO₂ NP and md-HAp micro-sized particles into the powder of conventional GIC Fuji IX did not result in improved compressive strength, breaking strength, and compressive modulus. This could be attributed to inadequate interaction between the added particles and the GIC matrix, most likely due to an inadequate p/l ratio that left many particles unreacted.

Author Contributions: Conceptualization, A.B. and A.I.; methodology, V.B.R., H.I.; and A.P.; validation V.B.R. and A.P.; formal analysis, A.I.; A.B. and M.P.; investigation, M.P.; H.I. and A.P.; resources, A.B. and H.I.; data curation, A.P.; writing—original draft preparation, A.I.; writing—review and editing, V.B.R.; A.B.; A.P. and M.P.; visualization, V.B.R.; A.P.; supervision, A.B.; project administration, A.I.; funding acquisition, A.B. All authors have read and agreed to the published version of the manuscript.

Funding: This research was funded by the Croatian Science Foundation, which is dedicated to the “Investigation and development of new micro and nanostructure bioactive materials in dental medicine” (BIODENTMED No. IP-2018-01-1719).

Institutional Review Board Statement: Not applicable.

Informed Consent Statement: Not applicable.

Data Availability Statement: The data that support the findings of this study are available from the corresponding author upon request.

Conflicts of Interest: The authors declare no conflict of interest.

References

1. Wilson, A.D.; Kent, B.E. A new translucent cement for dentistry. The glass ionomer cement. *Br. Dent. J.* **1972**, *132*, 133–135. [[CrossRef](#)] [[PubMed](#)]
2. Nicholson, J.W. Chemistry of glass-ionomer cements: A review. *Biomaterials* **1998**, *19*, 485–494. [[CrossRef](#)]
3. Fleming, G.J.P.; Farooq, A.A.; Barralet, J.E. Influence of powder/liquid mixing ratio on the performance of a restorative glassionomer dental cement. *Biomaterials* **2003**, *24*, 4173–4179. [[CrossRef](#)]
4. Algera, T.J.; Kleverlaan, C.J.; Prahl-Andersen, B.; Feilzer, A.J. The Influence of Environmental Conditions on the Material Properties of Setting Glass-Ionomer Cements. *Dent. Mat.* **2006**, *22*, 852–856. [[CrossRef](#)] [[PubMed](#)]
5. Andreeva, R. Usage of glass ionomer cements for reconstructions in the head region. *Int. Bull. Otorhinolaryngol.* **2020**, *16*, 38–41. [[CrossRef](#)]
6. Geyer, G.; Städtgen, A.; Schwager, K.; Jonck, L. Ionomeric cement implants in the middle ear of the baboon (*Papio ursinus*) as a primate model. *Eur. Arch. Otorhinolaryngol.* **1998**, *255*, 402–409. [[CrossRef](#)] [[PubMed](#)]

7. Brook, I.M.; Hatton, P.V. Glass-ionomers: Bioactive implant materials. *Biomaterials* **1998**, *19*, 565–571. [[CrossRef](#)]
8. Espelid, I.; Tveit, A.B.; Tornes, K.H.; Alvheim, H. Clinical behaviour of glass ionomer restorations in primary teeth. *J. Dent.* **1999**, *27*, 437–442. [[CrossRef](#)]
9. Šalinović, I.; Stunja, M.; Schauerperl, Z.; Verzak, Ž.; Ivanišević Malčić, A.; Brzović Rajić, V. Mechanical Properties of High Viscosity Glass Ionomer and Glass Hybrid Restorative Materials. *Acta Stomatol. Croat.* **2019**, *53*, 125–131. [[CrossRef](#)] [[PubMed](#)]
10. Mitra, S.B. Adhesion to dentin and physical properties of a light-cured glass-ionomer liner/base. *J. Dent. Res.* **1991**, *70*, 72–74. [[CrossRef](#)] [[PubMed](#)]
11. Elsaka, S.E.; Hamouda, I.M.; Swain, M.V. Titanium dioxide nanoparticles addition to a conventional glass-ionomer restorative: Influence on physical and antibacterial properties. *J. Dent.* **2011**, *39*, 589–598. [[CrossRef](#)] [[PubMed](#)]
12. Najeeb, S.; Khurshid, Z.; Zafar, M.S.; Khan, A.S.; Zohaib, S.; Marti, J.M.; Sauro, S.; Matinlinna, J.P.; Rehman, I.U. Modifications in Glass Ionomer Cements: Nano-Sized Fillers and Bioactive Nanoceramics. *Int. J. Mol. Sci.* **2016**, *17*, 1134. [[CrossRef](#)] [[PubMed](#)]
13. Bilić-Prčić, M.; Rajić, V.B.; Ivanišević, A.; Pilipović, A.; Gurgan, S.; Miletić, I. Mechanical Properties of Glass Ionomer Cements after Incorporation of Marine Derived Porous Cuttlefish Bone Hydroxyapatite. *Materials* **2020**, *13*, 3542. [[CrossRef](#)] [[PubMed](#)]
14. Yap, A.U.J.; Pek, Y.S.; Kumar, R.A.; Cheang, P.; Khor, K.A. Experimental studies on a new bioactive material: HA Ionomer cements. *Biomaterials* **2002**, *23*, 955–962. [[CrossRef](#)]
15. Moshaverinia, A.; Ansari, S.; Moshaverinia, M.; Roohpour, N.; Darr, J.A.; Rehman, I. Effect of incorporation of hydroxyapatite and fluoroapatite nanobioceramics into conventional glass ionomer cements (GIC). *Acta Biomater.* **2008**, *4*, 432–440. [[CrossRef](#)] [[PubMed](#)]
16. Cicciù, M.; Cervino, G.; Herford, A.S.; Famà, F.; Bramanti, E.; Fiorillo, L.; Lauritano, F.; Sambataro, S.; Troiano, G.; Laino, L. Facial Bone Reconstruction Using both Marine or Non-Marine Bone Substitutes: Evaluation of Current Outcomes in a Systematic Literature Review. *Mar. Drugs* **2018**, *16*, 27. [[CrossRef](#)] [[PubMed](#)]
17. Cibim, D.D.; Saito, M.T.; Giovani, P.A.; Borges, A.F.S.; Pecorari, V.G.A.; Gomes, O.P.; Lisboa-Filho, P.N.; Nociti-Junior, F.H.; Puppini-Rontani, R.M.; Kantovitz, K.R. Novel Nanotechnology of TiO₂ Improves Physical-Chemical and Biological Properties of Glass Ionomer Cement. *Int. J. Biomater.* **2017**, *2017*, 7123919. [[CrossRef](#)] [[PubMed](#)]
18. Garcia-Contreras, R.; Scougall-Vilchis, R.J.; Contreras-Bulnes, R.; Sakagami, H.; Morales-Luckie, R.A.; Nakajima, H. Mechanical, antibacterial and bond strength properties of nano-titanium-enriched glass ionomer cement. *J. Appl. Oral. Sci.* **2015**, *23*, 321–328. [[CrossRef](#)] [[PubMed](#)]
19. Garcia-Contreras, R.; Scougall-Vilchis, R.J.; Contreras-Bulnes, R.; Kanda, Y.; Nakajima, H.; Sakagami, H. Induction of prostaglandin E2 production by TiO₂ nanoparticles in human gingival fibroblast. *In Vivo* **2014**, *28*, 217–222.
20. Ahn, T.K.; Lee, D.H.; Kim, T.S.; Jang, G.C.; Choi, S.; Oh, J.B.; Ye, G.; Lee, S. Modification of Titanium Implant and Titanium Dioxide for Bone Tissue Engineering. *Adv. Exp. Med. Biol.* **2018**, *1077*, 355–368. [[CrossRef](#)] [[PubMed](#)]
21. Ivankovic, H.; Gallego Ferrer, G.; Tkalec, E.; Orlic, S.; Ivankovic, M. Preparation of highly porous hydroxyapatite from cuttlefish bone. *J. Mater. Sci. Mater. Med.* **2009**, *20*, 1039–1046. [[CrossRef](#)]
22. Figueiredo, M.M.; Gamelas, J.A.F.; Martins, A.G. *Characterization of Bone and Bone-Based Graft Materials Using FTIR Spectroscopy, Infrared Spectroscopy—Life and Biomedical Sciences*; Theophile, T., Ed.; InTech: Coimbra, Portugal, 2012; ISBN 978-953-51-0538-1. Available online: <http://www.intechopen.com/books/infrared-spectroscopy-life-and-biomedical-sciences/characterization-of-bone-and-bone-based-graft-materials-using-ftir-spectroscopy> (accessed on 10 June 2021).
23. ISO 9917-1. *Dentistry—Water-Based Cements—Part 1: Powder/Liquid Acid–Base Cements*; International Organization for Standardization: Geneva, Switzerland, 2007.
24. D’Alpino, P.H.; Lopes, L.G.; Pereira, J.C. Mechanical properties of dental restorative material: Relative contribution of laboratory test. *J. Appl. Oral. Sci.* **2003**, *11*, 162–167. [[CrossRef](#)]
25. Williams, J.A.; Billington, R.W. Increase in compressive strength of glass ionomer restorative materials with respect to time: A guide to their suitability for use in posterior primary dentition. *J. Oral. Rehab.* **1989**, *16*, 475–479. [[CrossRef](#)] [[PubMed](#)]
26. Gu, Y.W.; Yap, A.U.; Cheang, P.; Kumar, R. Spheroidization of glass powders for glass ionomer cements. *Biomaterials* **2004**, *25*, 4029–4035. [[CrossRef](#)] [[PubMed](#)]
27. Liufu, S.; Xiao, H.; Li, Y. Adsorption of poly(acrylic acid) onto the surface of titanium dioxide and the colloidal stability of aqueous suspension. *J. Colloid. Interface Sci.* **2005**, *281*, 155–163. [[CrossRef](#)]
28. Nicholson, J.W.; Sidhu, S.K.; Czarnecka, B. Enhancing the Mechanical Properties of Glass-Ionomer Dental Cements: A Review. *Materials* **2020**, *13*, 2510. [[CrossRef](#)] [[PubMed](#)]
29. Imataki, R.; Shinonaga, Y.; Nishimura, T.; Yoko Abe, Y.; Arita, K. Mechanical and functional properties of a novel apatite-ionomer cement for prevention and remineralization of dental caries. *Materials* **2019**, *12*, 3998. [[CrossRef](#)] [[PubMed](#)]
30. Yoshida, Y.; Van Meerbeek, B.; Nakayama, Y.; Snauwaert, J.; Hellemans, L.; Lambrechts, P.; Vanherle, G.; Wakasa, K. Evidence of chemical bonding at biomaterial-hard tissue interfaces. *J. Dent. Res.* **2000**, *79*, 709–714. [[CrossRef](#)] [[PubMed](#)]
31. Wilson, A.D.; Prosser, H.J.; Powis, D.R. Mechanism of adhesion of polyelectrolyte cements to hydroxyapatite. *J. Dent. Res.* **1983**, *62*, 590–592. [[CrossRef](#)] [[PubMed](#)]
32. Arita, K.; Yamamoto, A.; Shinonaga, Y.; Harada, K.; Abe, Y.; Nakagawa, K.; Sugiyama, S. Hydroxyapatite particle characteristics influence the enhancement of the mechanical and chemical properties of conventional restorative glass ionomer cement. *Dent. Mater. J.* **2011**, *30*, 672–683. [[CrossRef](#)]

-
33. Yap, A.U.; Pek, Y.S.; Cheang, P. Physico-mechanical properties of a fast-set highly viscous GIC restorative. *J. Oral. Rehabil.* **2003**, *30*, 1–8. [[CrossRef](#)] [[PubMed](#)]
 34. Pereira, L.C.; Nunes, M.C.; Dibb, R.G.; Powers, J.M.; Roulet, J.F.; Navarro, M.F. Mechanical properties and bond strength of glass-ionomer cements. *J. Adhes. Dent.* **2002**, *4*, 73–80. [[PubMed](#)]